Rotaxanes as ligands: from molecules to materials

Stephen J. Loeb

Received 6th September 2006
First published as an Advance Article on the web 20th November 2006
DOI: 10.1039/b605172n

This *tutorial review* documents the discovery and application of the supramolecular template (1,2-bis(pyridinium)ethane)⊂(24-crown-8) for preparing interlocked molecules. Focus is on the supramolecular chemistry of the pseudorotaxanes formed with various pyridinium axles and crown ether wheels and how this particular class of mechanically linked molecule has been (i) used to construct rudimentary molecular machines such as molecular shuttles and flip switches, (ii) used as ligands for coordination chemistry and (iii) used to create metal–organic framework (MORF) materials.

1. Interpenetrated and interlocked molecules

1.1 Introduction

A variety of strategies now exist for the preparation of mechanically interlocked molecules such as rotaxanes and catenanes. From a supramolecular point of view, this often involves non-covalent interactions between a linear "axle" and a cyclic "wheel" to form an interpenetrated adduct known as a [2]pseudorotaxane. This supramolecular assembly can then be converted to a permanently interlocked [2]rotaxane by capping with bulky end groups or to a [2]catenane by linking the two ends of the linear axle. Although a wide array of complementary components capable of [2]pseudorotaxane formation can be envisioned, there are only a few supramolecular systems that are efficient at threading and amenable to significant structural modification. Not surprisingly, it is this handful of versatile systems that have been exploited to create families of mechanically linked molecules, molecular machines and nanoscale devices.[1]

Department of Chemistry & Biochemistry, University of Windsor, Windsor, Ontario, Canada N9B 3P4. E-mail: loeb@uwindsor.ca; Fax: +1-519-973-7098; Tel: +1-519-253-3000

Stephen J. Loeb

Steve Loeb was born in London, UK. He completed a PhD in chemistry at the University of Western Ontario and after postdoctoral work at the University of Alberta and a teaching stint at the University of Winnipeg, moved to the University of Windsor in 1990 where he is currently a Professor of Chemistry. He is a Fellow of the Chemical Institute of Canada and the Canada Research Chair in Supramolecular Chemistry and Functional Materials. His primary research area is interlocked molecules and their use in the construction of molecular machines and mechanically linked materials. He also has interests in the design of new inorganic receptors for anions.

1.2 The (1,2-bis(pyridinium)ethane)⊂(24-crown-8) template

In 1998, we reported in a preliminary communication that 1,2-bis(pyridinium)ethane, (**BPE**)† "axles" and 24-membered crown ether "wheels" could combine to form [2]pseudorotaxanes.[2] The inspiration for this design came from Stoddart's pioneering observation that paraquat (**PQT**)$^{2+}$ could thread through the cavity of the macrocycle bis(paraphenylene)-34-crown-10 (**BPP34C10**) to form the stable [2]pseudorotaxane [(**PQT**)⊂(**BPP34C10**)]$^{2+}$.[3] In the X-ray structure of this supramolecular adduct, the (**PQT**)$^{2+}$ dication is tilted away from being perpendicular to the cavity of **BPP34C10** by ~62°; Fig. 1. This is presumably in order to maximise electrostatic $N^+\cdots O$ interactions and form $CH\cdots O$ hydrogen bonds to accompany a significant π-stacking component. We noted that the $N^+\cdots N^+$ distance in (**PQT**)$^{2+}$ is ~7.00 Å, while in the isomeric (**BPE**)$^{2+}$ dication it is shortened considerably to ~3.75 Å. Examination of CPK and computer models suggested that the interaction of this new axle with smaller 24-membered crown ethers wheels would give rise to an interpenetrated structure as shown in Fig. 1 (bottom).

Detailed studies showed that the combination of linear **BPE** axles and 24-membered crown ether wheels (24-crown-8, **24C8**; dibenzo-24-crown-8, **DB24C8**; dinaphtho-24-crown-8, **DN24C8**) is an efficient and versatile templating motif for the formation of [2]pseudorotaxanes. Solution and solid state evidence demonstrated that these interpenetrated adducts are held together by $N^+\cdots O$ ion–dipole interactions, a series of eight $CH\cdots O$ hydrogen bonds and, where possible, significant π-stacking interactions between electron-poor pyridinium rings and electron-rich catechol rings as depicted in Fig. 2.[4]

---

† The acronym **BPE** is used throughout this review to indicate the general class of "axle" derived from the "1,2-bis(pyridinium)ethane" structure. Strictly speaking this is also the name of the parent axle for which X = Y = H in Fig. 2. (**BPE**)$^{2+}$ is used when the structure of the actual molecular species is being described as in section 1.2. Alternatively, and probably more correctly, this compound could be called 1,1′-(1,2-ethanediyl)bis(pyridinium).

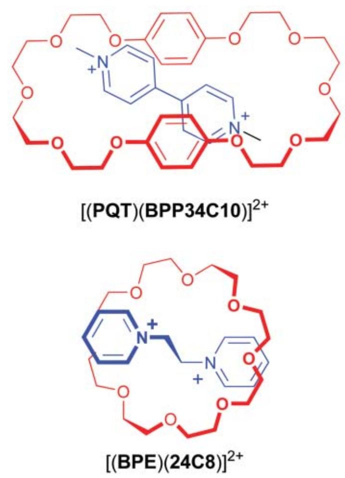

[(**PQT**)(**BPP34C10**)]$^{2+}$

[(**BPE**)(**24C8**)]$^{2+}$

Fig. 1 The two isomeric pyridinium dications (**PQT**)$^{2+}$ and (**BPE**)$^{2+}$ have the same basic set of components for non-covalent interactions but the arrangement of these units on the axle gives rise to fundamentally different [2]pseudorotaxane motifs with different sized crown ethers.

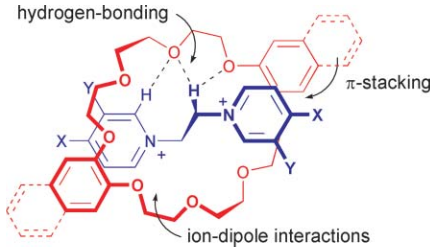

Fig. 2 A schematic example of a [2]pseudorotaxane showing the non-covalent interactions that hold the **BPE** axle (blue) and crown ether wheel (red) together in an interpenetrated arrangement. The strength of these interactions can be fine tuned by the addition of electron-withdrawing groups (EWG) or electron-donating groups (EDG) (X, Y) and the presence of aromatic groups (benzo, naphtho) on the crown ether.

The strength of the non-covalent interactions could be controlled by varying the substituents on the axle pyridinium rings. In particular, an EWG provides increased hydrogen bonding and electrostatic interactions and therefore an increase in the stability of the system. Unlike alkylammonium axles, which show the highest association constants with **24C8**, the new **BPE** motif exhibits very significant contributions from π-stacking and higher association constants with **DB24C8**. We have also shown that the use of a wheel with an extended π-system, such as **DN24C8**, results in a further increase in stability. Association constants for this series of [2]pseudorotaxanes ranged from 10 to 4700 M^{-1} in MeCN-d_3 at 298 K.[4]

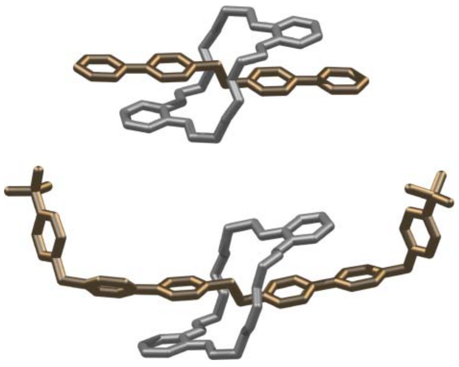

Fig. 3 The X-ray crystal structures of (top) the [2]pseudorotaxane derived from a combination of **A1** (gold) and **DB24C8** (silver) and (bottom) the [2]rotaxane formed by alkylation with *t*-Bu-benzyl groups.

1.3 [2]Rotaxanes

The formation of [2]rotaxanes from [2]pseudorotaxanes involves the incorporation of bulky capping groups to prevent unthreading of the axle component from the wheel unit. This "threading-followed-by-capping" method has given rise to a number of synthetic capping strategies such as alkylation of amines and phosphines, ester, carbonate and acetal formation, oxidative coupling, cycloaddition, and Wittig reactions.[5] We prepared the axle 1,2-bis(4,4′-bipyridinium)ethane (**A1**) with terminal pyridine groups. This allowed for the straightforward incorporation of a capping group by direct alkylation of the terminal pyridines; see Fig. 3. The *tert*-butylbenzyl group was employed as the cap as it was shown previously[4] that a pyridinium ring with a *t*-Bu substituent could not pass through **DB24C8**.[6]

1.4 [$n > 2$]Rotaxanes

Polyrotaxanes and polycatenanes are supramolecular polymers that contain macromolecular architectures built with mechanical linkages. Interest in these systems can be attributed to the fundamental role that interlocked components might play in the mechanical properties of polymers. Dendrimers and hyperbranched macromolecules based on interlocked components have also attracted recent attention as models for supramolecular polymers.[7]

We were particularly interested in dendrimers in which all the branching points of the macromolecule are mechanical linkages. These can be constructed by either threading multiple ring components onto branches attached to a single core (type A) or threading multiple axles on to rings appended to a central core (type B).[8] Initially, we prepared extended axles containing two **BPE** type binding sites. Threading multiple units of **DB24C8** onto the axle, followed by capping with *t*-Bu-benzyl groups gave type A [3]rotaxanes.[9]

Type B dendrimeric polyrotaxanes were prepared using multi-site crown ethers and **A1** axles; see Fig. 4 for an example.[10] The product distribution of branched [*n*]rotaxanes observed gave a measure of the efficiency of the threading process. The size of the core could be a single benzene ring but this was only practical for the formation of two branches as the two crowns needed to be positioned away from each other in the 1,4-orientation to minimise inhibitory interactions.[10] Attaching crown units to a central benzene ring allowed the formation of a larger [4]rotaxane with three branches. The efficiency of the threading steps decreased sequentially and was attributed to three factors: (1) steric interactions between an already complexed crown ether site (pseudorotaxane or rotaxane) and the new incoming axle; (2) electrostatic repulsions between an existing rotaxane axle and the new incoming

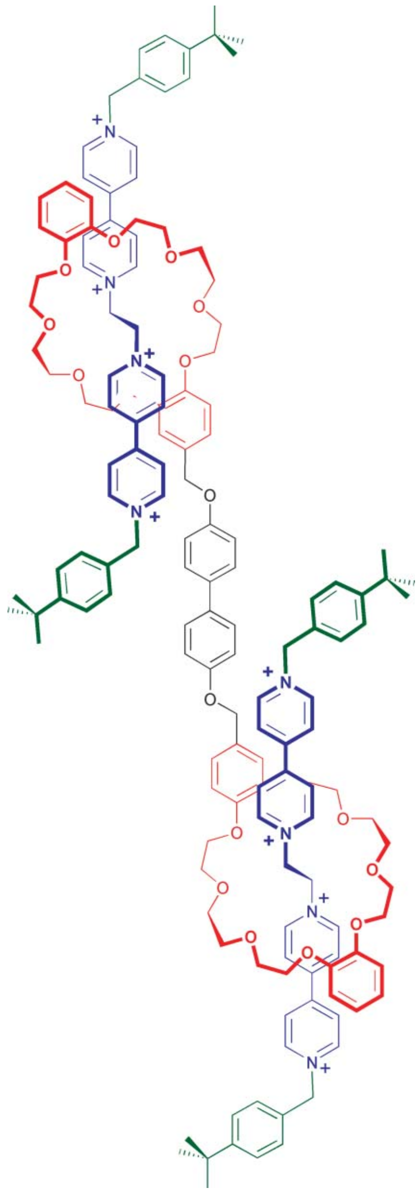

Fig. 4 The bis(crown) ether with a biphenyl spacer allows formation of a [3]rotaxane using **A1** capped with *t*-Bu-benzyl groups.

axle; and (3) partial occupation of the unoccupied crown ether recognition elements by a neighbouring rotaxane unit.[10]

1.5 [3]Catenanes: an example of host–guest templating

The synthesis of complex interlocked assemblies such as $[(n > 2)]$catenanes, $[(n > 2)]$molecular necklaces and $[(n > 2)]$rotacatenanes remains a considerable challenge for supramolecular chemists.[1] One of the major problems is that, regardless of design, there is always the requirement of forming at least one large ring during the self-assembly process. A potential strategy to aid ring-closure involves the use of an external template, for example, a guest for a host catenane. During our studies on the [(**BPE**)⊂(**24C8**)] templating motif, we discovered a unique a one-step, self-assembly procedure for the preparation of [3]catenanes utilising a terphenyl spacer unit that used **DB24C8** as a very efficient template for the assembly of the [3]catenane containing this crown.[11] The X-ray structure in Fig. 5 shows how **DB24C8** can act as a guest for the [3]catenane host, an interaction that can act to template the cyclisation reaction and produce [3]catenane in good yield. The yield of the [3]catenane with **DB24C8** was twice that with any other crown ether studied (**24C8**, **B24C8**, **N24C8**, **DN24C8**) as only **DB24C8** was a suitable guest.

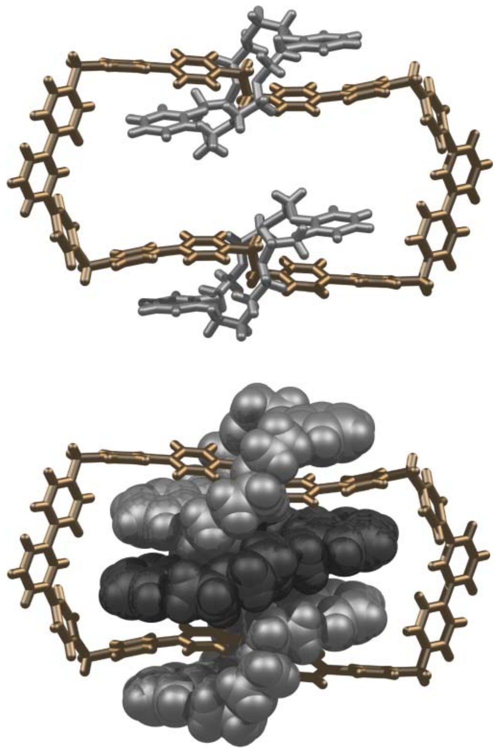

Fig. 5 X-Ray structures of (top) the [3]catenane and (bottom) the [3]catenane host with an equivalent of **DB24C8** as the guest.

2. Molecular machines

2.1 Introduction

Control over the relative position and motion of components in interpenetrated or interlocked molecules can impart machine-like properties at the molecular level. Examples include threading and unthreading of a [2]pseudorotaxane, translation of the macrocycle in a [2]rotaxane molecular shuttle, rotation of the rings in a [2]catenane, or reorientation (flipping, pirouetting) of the cyclic wheel in [2]rotaxanes.[12]

2.2 Controlling threading and unthreading

During our study of [2]pseudorotaxane formation between **BPE** axles and 24-membered crown ether wheels, we noted that the presence of a strong EDG, such as NH_2, dramatically reduced the association constant.[4] This was attributed to a reduction in the acidity of the hydrogen bonding groups and a reduction in the charge at the pyridinium nitrogen due to contributions from an unfavourable resonance form. We then prepared an axle which could be represented by two resonance forms having dramatically different structures and charge distributions. This new axle had the structure of an organic

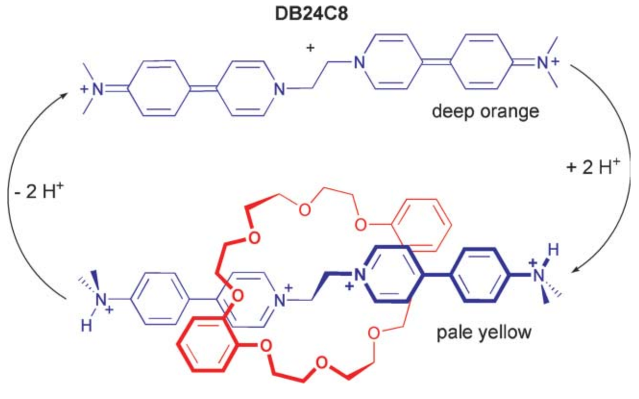

Fig. 6 A schematic representation of the threading and unthreading process driven by alternating acid and base using an ICT axle.

D–π-A–π-D chromophore with two terminal donor groups (*N*,*N*-dimethylamino) and an inner acceptor group (bis(pyridinium))ethane giving rise to an intramolecular charge transfer (ICT). It was possible to turn OFF the ICT by addition of a Lewis acid. X-Ray crystal structures of the neutral and protonated forms as well as DFT (B3LYP) calculations verified the predicted resonance structures and electronic differences.[13]

A substantial increase in association constant was observed for the protonated form compared to the unprotonated form. An ICT band with $\lambda_{\max}$ at 447 nm was observed in the absorption spectrum but this intense orange colour was completely eliminated upon addition of acid. The colourless, protonated axle then formed a [2]pseudorotaxane with **DB24C8**, which gave rise to a pale yellow coloration due to the weak charge-transfer interaction typical of [(**BPE**)⊂(**DB24C8**)] pseudorotaxanes; see Fig. 6.

The linking of this mechanical action of [2]pseudorotaxane formation to a significant colour change can be described as a NOT logic gate since the threading of the two components to form the interpenetrated molecule is signalled by the loss of the orange colour.

2.3 Molecular shuttles

The transformation of mechanically linked molecules such as [2]rotaxanes and [2]catenanes into molecular machines requires the synthesis of systems with two or more distinct molecular arrangements (co-conformations).[12] One of the most widely studied of these is the molecular shuttle pioneered by Stoddart *et al.*.[12] In a molecular shuttle, two different recognition sites are present on the axle for the binding of a single macrocyclic wheel. The two states are translational isomers, related by the relative positioning of the two interlocked components.

We utilised the axles from our [3]rotaxane study[14] to create molecular shuttles containing two binding sites of the **BPE** type for a single molecule of **DB24C8**.[34] Since only one set of ^{1}H NMR resonances was observed for the axles at room temperature, it was concluded that the **DB24C8** molecules were undergoing fast exchange between the two binding sites. From VT-NMR spectral data it was determined that the rate of exchange between the two sites was on the order of 200–300 Hz. For the unsymmetrical example shown in Fig. 7, the ratio of site occupancy was determined to be 2 : 1.

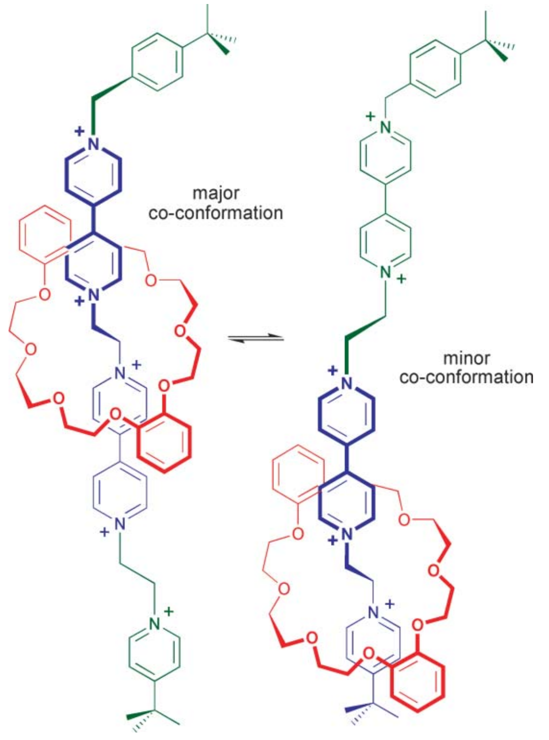

Fig. 7 A dynamic molecular shuttle based on two different **BPE** type recognition sites.

In order to actually control the motions of the components in these molecular shuttles, the **BPE** site was combined with an alkylammonium site which can be turned ON and OFF by protonation and deprotonation.[15] Fig. 8 shows a molecular shuttle that operates as a bistable switch in chloroform solution by the sequential addition of acid and base. When the amine site is unprotonated there is no recognition element to interact with the crown ether. Upon protonation, a

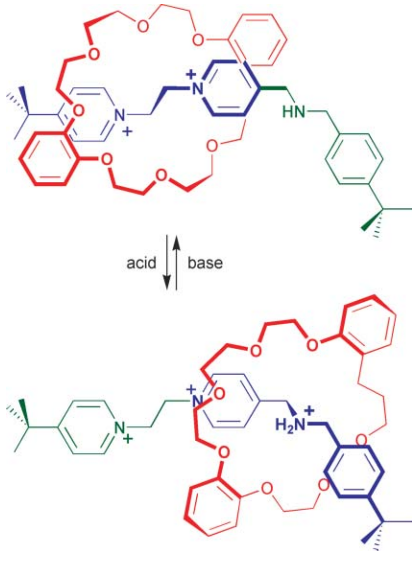

Fig. 8 A molecular shuttle containing both **BPE** and alkylammonium recognition sites that can be controlled by the addition of acid and base.

competition is established between the two sites, which is dominated totally by the secondary ammonium ion recognition in a non-polar solvent like chloroform but is dynamic in a more polar environment such as acetonitrile.

2.4 Flip switches

Recently, we demonstrated the existence of a new set of positional isomers based on [2]rotaxanes which contain a single recognition site but have different end groups on both the **BPE** axle and crown ether wheel (benzonaphtho-24-crown-8, **BN24C8**). The relative positioning of the two interlocked components produces two co-conformations and their re-orientation is reminiscent of a mechanical "flip switch".[16]

^{1}H NMR spectroscopy was used to determine that the populations of the two co-conformations were dependent upon the relative degrees of π-stacking between axle and wheel. Since solvent polarity is known to have a profound influence on intramolecular face-to-face π-stacking between aromatic rings,[17] we studied a system with two different planar pyridinium groups of different surface area and demonstrated that the ratio of co-conformational isomers could be tuned by solvent polarity; Fig. 9. The ratio of isomers showed an increase in π-stacking of the naphtho group with the 4,4′-bipyridinium group in more polar solvents.

We had also observed this phenomenon when using a novel pyridinium–phosphonium axle but were unable to control the switching behaviour.[18]

3. Interlocked molecules as ligands

3.1 [2]Pseudorotaxanes as ligands

Almost any metal complex with a single open coordination site is bulky enough to be used as an effective cap and form a metal-based [2]rotaxane. Our initial study involved using the axle **A1** and **DB24C8** to pre-form the [2]pseudorotaxane ligand **RL1** and then capping it with the palladated pincer fragment [Pd($C_6H_3(CH_2SPh)_2$)]$^+$.[6] The ^{1}H NMR spectrum of the reaction mixture showed quantitative formation of the metal capped [2]rotaxane, which could be isolated from solution by crystallisation; an X-ray structure verified the interlocked nature of the product. Subsequently, it was shown that the metal-containing caps could be larger, more sophisticated units such as the porphyrin complex [Ru(CO)(TTP)][19] (TTP = tetraphenylporphyrin) or simple anionic metal fragments such as [MBr_3] (M = Mn, Co).[5] The X-ray structures of the PdS_2 and $CoBr_3$ capped complexes are shown in Fig. 10.

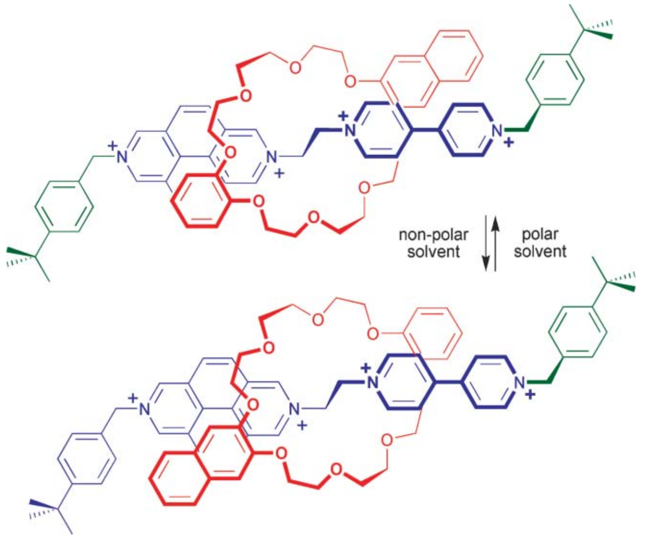

Fig. 9 [2]Rotaxanes containing a **BPE** recognition site in which both the axle and wheel have different end groups can exist in two different co-conformations that depend on the orientation of the components. The preference for a particular co-conformation is dependent upon π-stacking interactions and can be controlled by solvent polarity.

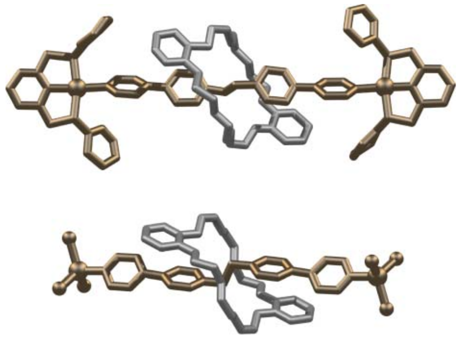

Fig. 10 The X-ray crystal structures of the [2]rotaxanes derived from a combination of **A1** (gold) and **DB24C8** (silver) capped by (top) the palladated pincer fragments [Pd($C_6H_3(CH_2SPh)_2$)]$^+$ and (bottom) the anionic fragments $CoBr_3$.

3.2 [2]Rotaxanes as ligands

One of the shortcomings of a self-assembly strategy for metal ion incorporation is that conditions for formation of the metal–ligand bonds must be compatible with maintaining the weaker non-covalent interactions between axle and wheel. A simple modification that circumvented this problem was replacement of one of the monodentate pyridine donors of **A1** with a multidentate terpyridine group to give new axle **A2**. The new axle was then incorporated into a permanently interlocked [2]rotaxane, **RL2**, prior to coordination; see Fig. 11 (top).

We then studied the coordination chemistry of **RL2** with Fe(II)[20] and Ru(II).[21] Since **RL2** is already a [2]rotaxane, the conditions under which coordination to a metal centre are conducted do not effect the integrity of the mechanical linkage. For example, the Ru(II) complexes were prepared at reflux in polar solvents with no decomposition of the [2]rotaxane ligand.

A detailed investigation of a series of these Ru(II) complexes (see Fig. 11, bottom) showed some unique photophysical properties that could be fine tuned by varying the nature of the crown ether.[21] This synthetic approach, therefore, has the potential to greatly expand the conditions under which metal complexes with mechanical linkages can be prepared and should lead to the incorporation of a wide variety of metal ions with unique electronic, magnetic or photophysical properties.[22]

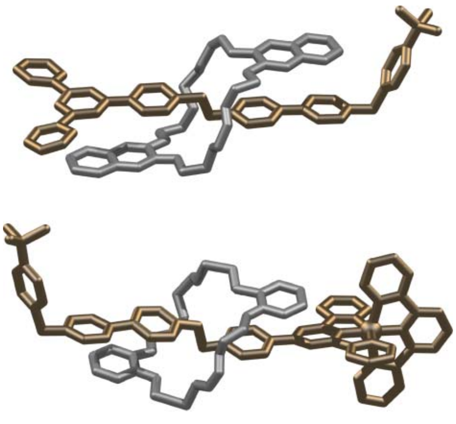

Fig. 11 The X-ray crystal structures of (top) the ligand **RL2**, containing a terpyridine chelating axle capped with a *t*-Bu-benzyl group (gold) and **DB24C8** (silver) and (bottom) the coordination complex formed with **RL2** and an equivalent of $[Ru(terpy)]^{2+}$ (terpy = 2,2′:6′,2″-terpyridine).

4. Materials from interlocked molecules

4.1 Metal–organic rotaxane frameworks (MORFs)

Although a great deal of information about the fundamental properties of mechanically interlocked molecules has been derived from solution studies,[23–26] there still need to be methods for imposing order in these systems. Some ideas that have been studied are (i) attachment to surfaces,[27] (ii) tethering between electrodes,[28] (iii) incorporation into organic polymers[29] or dendrimers[8] and (iv) assembly into the repeating framework of a crystalline lattice.[30] The ultimate goal is to produce materials that contain functional components that are individually addressable and controllable. We are interested in the solid state and, in particular, the formation of crystalline materials we have termed metal–organic rotaxane frameworks (MORFs).[31]

The use of simple [2]rotaxanes as linkers in MORF materials should provide a blueprint for the eventual organising of molecular machines into 3-dimensional frameworks. The challenge is to design appropriate ligands and devise protocols for self-assembly synthesis and crystallisation. One defining attribute of a conventional metal–organic framework (MOF) material is the ability to modify the linker unit by organic synthesis.[31] With MORFs, an additional degree of flexibility is available as the rotaxane linker can be modified by retaining the axle unit but exchanging the wheel component. This supramolecular modification can potentially be used to tune the internal properties of the material.[32]

4.2 One-dimensional MORFs

The evolution from a [2]rotaxane capped with metal fragments to a 1D MORF was straightforward. Mixing **A1** with an excess of **DB24C8** in MeCN resulted in a solution which contained an equivalent of the ligand **RL1**. Diffusion of a solution of **RL1** (as the BF_4 salt) into an MeCN solution of $[M(H_2O)_6][BF_4]_2$ (M = Co, Zn) resulted in isolation of crystalline material with formula $\{[Co(H_2O)_2(MeCN)_2(\mathbf{RL})][BF_4]_4\cdot(MeCN)_2\cdot(H_2O)_2\}_x$ (yields: 71% Co, 92% Zn).

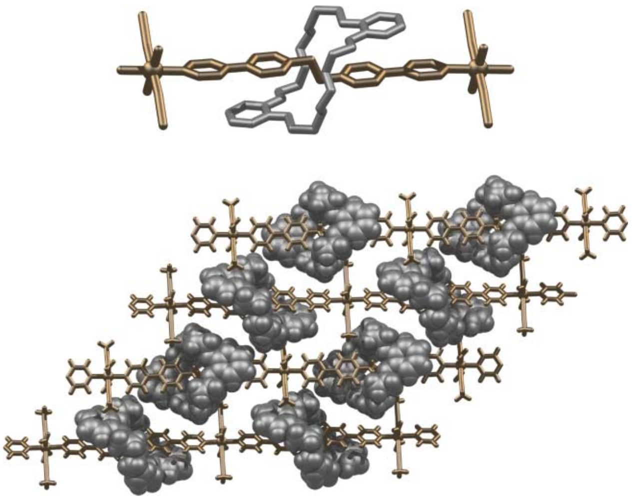

Fig. 12 The X-ray crystal structure of a 1D MORF with Co(II) ion nodes and **RL1** linkers showing (top) a single repeating unit and (bottom) four parallel strands.

Fig. 12 (top) shows that the use of Co(II) ions in the presence of a coordinating solvent such as MeCN results in an octahedral coordination sphere comprised of two equivalents of **RL1**, two MeCN molecules and two water molecules, with each set of ligands having a *trans* orientation. The result is a coordination polymer in which every linker is a [2]rotaxane.

The linearity of the framework is due to the fact that **A1** can adopt only an *anti* conformation at the central ethylene unit when threaded through **DB24C8**. This, combined with a *trans* geometry at the metal ion, produces a linear 1D MORF with Co···Co 22.1 Å.[33] This polymer can be viewed as a metal–ligand "wire" in which the crown ethers act as a protective coating analogous to the use of long-chain hydrocarbons attached to phosphine ligands to surround metal polyacetylene linkages.[34] This MORF also contains infinite channels parallel to the polymer chains which are filled with anions and solvent. Fig. 12 (bottom) shows several strands of the framework. It is likely that the girth of this rotaxane ligand contributes to both the parallel organisation of the chains as well as the channels between them. As evidence for this, we have crystallised two 1D polymers utilising only **A1** as the linker. In both cases, we observed a classic herringbone pattern; there were no parallel alignments of chains and neither compound contained void channels for solvent occlusion.[35]

4.3 Two-dimensional MORFs

Since the linear 1D MORFs contained an octahedral metal ion in which the ancillary ligands were solvent molecules, we reasoned it should be possible to induce higher orders of dimensionality by employing a greater amount of **RL1** in a non-coordinating solvent. The reaction of two equivalents of **A1** (as the BF_4 salt) with four equivalents of **DB24C8** and one equivalent of $[M(H_2O)_6][BF_4]_2$ (M = Cu, Cd, Ni) in $MeNO_2$ produced X-ray quality crystalline material (average yields ~80%).[33] Fig. 13 (top) shows how the use of these metal ions in a non-coordinating solvent allows for an octahedral coordination geometry comprising four **RL1** linkers in a square planar arrangement, along with one water molecule and

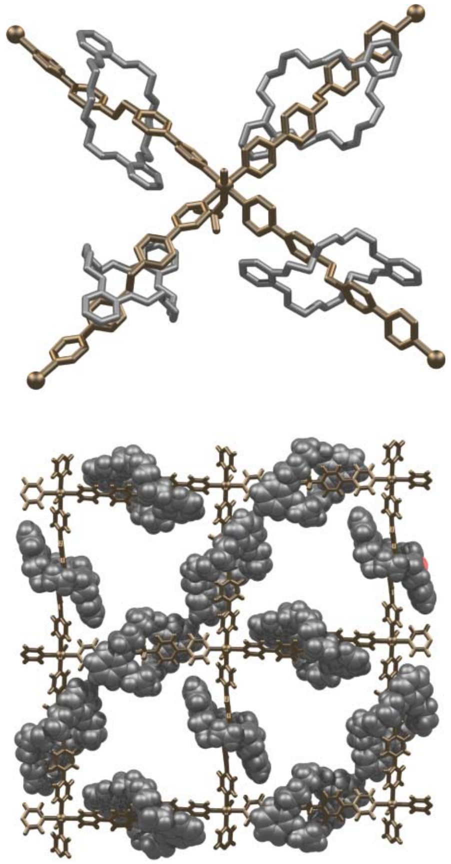

Fig. 13 The X-ray crystal structure of a 2D MORF with Cd(II) ion nodes and **RL1** linkers showing (top) the coordination sphere around a single metal ion and (bottom) a portion of the 2D square net.

one coordinated BF_4 anion. Fig. 13 (bottom) shows how propagation of these units results in a 2D MORF with square nets and formula $\{[Cd(H_2O)(BF_4)(\mathbf{RL1})_2][BF_4]_5(MeNO_2)_{15}\}_x$. The sides of the square are defined by Cd···Cd distances of 22.2 Å. The interlayer spacings are 12.0 and 10.0 Å, with the layers stacked in a pattern that gives rise to an open framework material with large infinite channels lined with crown ethers. The channels are filled with anions and solvents; there are 15 molecules of $MeNO_2$ per Cd(II) ion. Calculations estimate that the accessible void space occupied by anions and solvent is 50%; 38% for solvent only.[33]

4.4 Three-dimensional MORFs

Regardless of the metal-to-ligand ratio employed, a two dimensional square net was the highest order MORF that could be attained using **RL1** as a bridging ligand. We ascribed the failure to obtain 3D frameworks to the hindrance involved in trying to place six sterically-demanding ligands around a single transition metal ion. In order to avoid crowding at the metal centre, we made two changes. (1) We synthesised the bis(*N*-oxide) analogue of **A1** to give a new axle **A3**, which allowed the formation of a new linker **RL3** and (2) we employed larger lanthanide metal ions.

Three equivalents of **A3** (as the OTf salt) were reacted with nine equivalents of **DB24C8** and one equivalent of $[M(OTf)_3]$ (M = Sm, Eu, Gd, Tb) in MeCN. X-Ray quality crystalline material was produced in moderate yield (average yields ~50%). Fig. 14 (top) shows that the use of Ln(III) ions as nodes results in an eight-coordinate metal centre with a square *anti*-prismatic geometry comprised of six **RL3** linkers, one water molecule and one coordinated triflate anion.[36] Fig. 14 (bottom) shows how propagation of these units results in 3D MORFs with formula $\{[M(H_2O)(OTf)(\mathbf{RL3})_3][Cl][OTf]_7\cdot(2MeCN)\}_x$, (M = Sm, Eu, Gd, Tb) in which every linker is a [2]rotaxane. The edges of the "cube" are defined by Sm···Sm distances of ~23.5 Å. Although the 3D cavity of this framework has a volume of ~10 000 $Å^3$, this apparently void space is filled by the single interpenetration of a parallel net. This is an obvious side-effect of employing the longer axles and creating elongation of the metal–metal distance. This creates an expanded cavity with larger "windows" which can accommodate the girth of the [2]rotaxane ligand and allow interpenetration to occur.

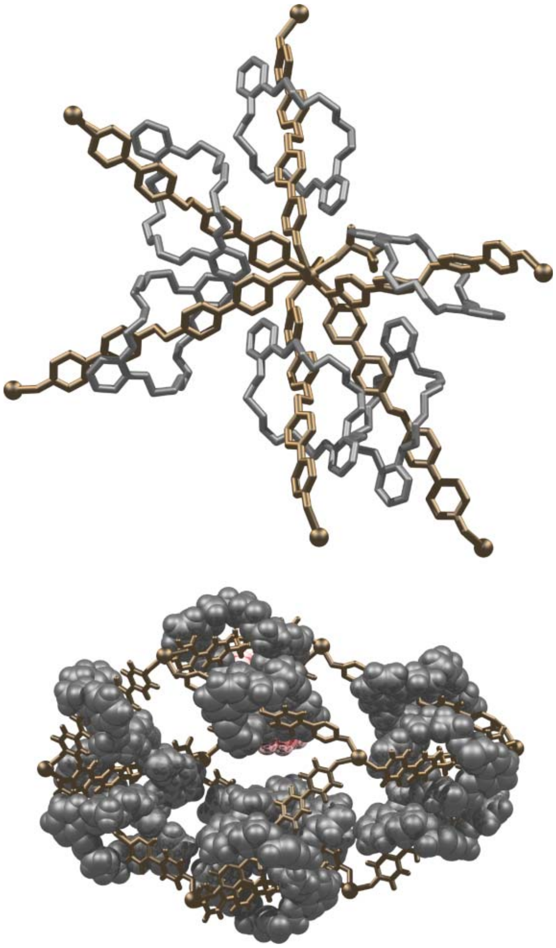

Fig. 14 The X-ray crystal structure of a 3D MORF with Sm(III) ion nodes and **RL3** linkers showing (top) the coordination sphere around a single metal ion and (bottom) a portion of the α-Po type framework.

An isomorphous series of 3D MORFs (Sm, Eu, Gd, Tb) based upon eight coordinate metal centres was possible, but changing to a smaller lanthanide ion, Yb(III) (2.40 Å *vs.* 2.51 Å for Tb), yielded a completely different MORF. A material with formula $\{[Yb(OTf)(\mathbf{RL3})_3][Cl][OTf]_7\}_x$, was isolated in moderate yield using the same diffusion procedure used to produce the other 3D MORFs. In this case, a seven-coordinate pentagonal bipyramidal geometry was adopted by the smaller Yb(III) centre. Five *N*-oxide based rotaxanes occupy the equatorial sites of the pentagonal plane, with a sixth rotaxane and a single triflate ion positioned in the axial sites; Fig. 15 (top). Upon reducing the size of the Ln(III) node, a single water molecule is removed and the coordination number decreased from 8 to 7. This subtle change has a dramatic effect on the nature of the resulting MORF structure.[36] Since the novel seven-coordinate geometry at Yb(III) contains a pentagonal equatorial plane and close-packed tiling in two dimensions with pentagons is impossible, it was interesting to see how this dilemma was circumvented. What occurs is, each *N*-oxide ligand ''bends'' at the Yb–O–N linkage so a (3/4,5) net is formed, which solves the problem by utilising a combination of alternating triangles and squares rather than pentagons. Until very recently, this two dimensional pattern was unknown in chemical systems.[37] Fig. 15 (bottom) shows the tiling in the pentagonal plane. This network propagates one step further into a full 3D MORF by pillaring to alternating layers utilising the sixth **RL3** ligand in the apical position. This results in a previously unknown chemical topology which takes the form of a (3/4/6,6) 6-connected net comprised of triangles, squares and hexagons. The square openings are used for interpenetration as this is not possible through the more crowded triangular cavities.

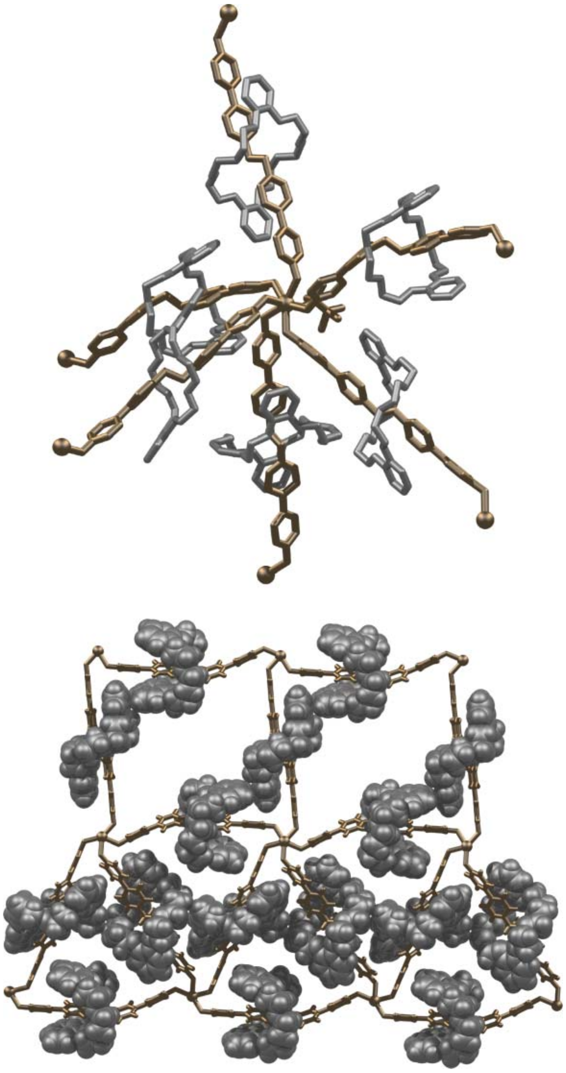

Fig. 15 The X-ray crystal structure of a 3D MORF with Yb(III) ion nodes and **RL3** linkers showing (top) the coordination sphere around a single metal ion and (bottom) the unique 2D network comprised of square and triangular units.

4.5 Controlling the dimensionality of a MORF

Attempts to construct a 3D MORF with **RL3** using smaller transition metal ions such as Cd(II) yielded a polyrotaxane but not the desired 3D framework. Instead, a 2D network was created with only one of the directions utilising **RL3** and the other simply employing **A3** as a linker with no crown ether wheel.[38] Fig. 16 (top) shows the basic coordination sphere around the Cd(II) centre.

The X-ray crystal structure of the MORF material shows that the solid has the formulation {[Cd(**RL3**)(**A3**)(OTf)$_2$][OTf]$_4$(MeNO$_2$)$_4$}$_n$. The Cd(II) metal centres adopt an octahedral geometry with three different pairs of ligands in an all *trans* arrangement. Two rotaxane ligands and two naked axles define a square plane while two triflate anions are in the axial positions. This is similar of the Cd(II) MORF prepared using the pyridine-based rotaxane ligand **RL1**. In that structure, the cavities of the grid were aligned to produce large channels filled with solvent.[33] However, in this new structure, each cavity is filled by crown ethers from the layers above and below. The network is actually reminiscent of the 1D MORF structure based on Co(II) or Zn(II) and **RL1** as it

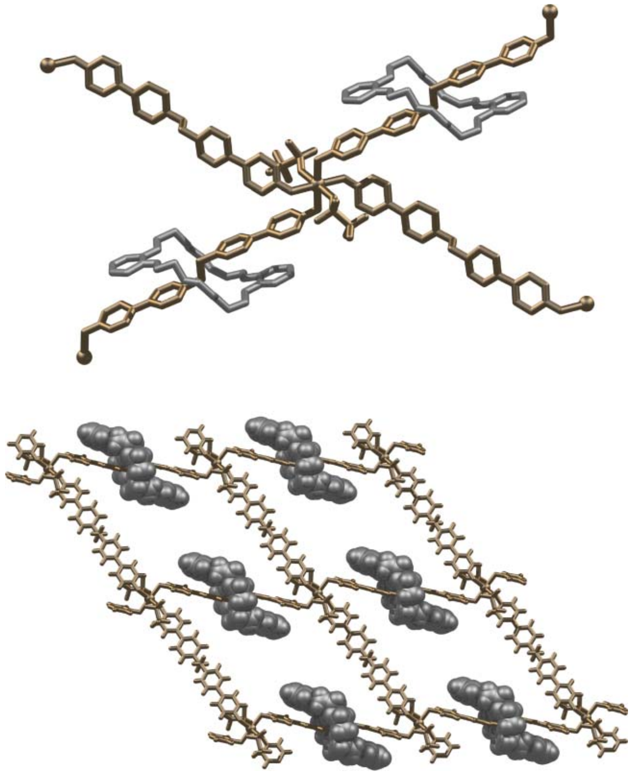

Fig. 16 The X-ray crystal structure of the pillared 1D MORF with Cd(II) ion nodes, **RL3** linkers and **A3** pillars showing (top) the coordination sphere around a single Cd(II) ion and (bottom) a portion of the polar 2D network.

can thought of as a pillared 1D MORF. That is, the two *trans* oriented **RL3** linkers coordinate to the Cd(II) centre in one dimension while the two **A3** molecules pillar the polyrotaxane strands in the second dimension.

Finally, a property of this new MORF that is intriguing is its crystallisation in the non-centrosymmetric space group, *P*1. All the crown ether wheels are oriented in the same fashion along each strand of each grid. This is significant as it may be possible to replace **DB24C8** with substituted crown ethers and thus orient all the wheel dipoles in the same direction by virtue of their entrapment on the metal–ligand grid. This has potential as a novel method for creating NLO materials by supramolecular modification.

4.6 Frameworks using hydrogen-bonding

Since we had success in using metal ions as nodes to build MORFs we looked at the possibility of using hydrogen-bonding for the systematic preparation of solid-state materials that contain mechanical linkages. In this vein, we have shown that H^+ can be used in place of a metal ion to form polymeric systems with formula $\{[(\mathbf{RL1}\text{-}H_2)(\mathbf{DB24C8})][OTf]_4\}_x$ *via* hydrogen bonding.[39] In a single stranded 1D MORF structure, the di-protonated [2]pseudorotaxane (**RL1**-H_2) acts as the H-bond donor, while an extra equivalent of **DB24C8** acts as the H-bond acceptor. Fig. 17 (top) shows this H-bonded pair, while Fig. 17 (bottom) shows how this motif extends into a polymeric structure with parallel strands.

5. The future: functional MORF materials

5.1 Robust frameworks

All of the MORF materials prepared to date show the same basic stability. They are highly crystalline materials that occlude solvent to some degree and each loses some portion of the trapped solvent rapidly upon removal from the mother liquor at room temperature. Thermogravimetric analysis showed that all residual solvent was removed after heating to ~100 °C. Each MORF studied then showed a stable phase until ~225–250 °C, at which point decomposition of the metal–ligand framework was indicated by loss of **DB24C8**. It should be noted that the interlocked crown ether, although it is originally held in place by weak non-covalent bonds, can only be removed by breaking a bond in the metal–ligand backbone. Thus, the loss of **DB24C8** is actually a sensitive and unambiguous detection of framework breakdown.

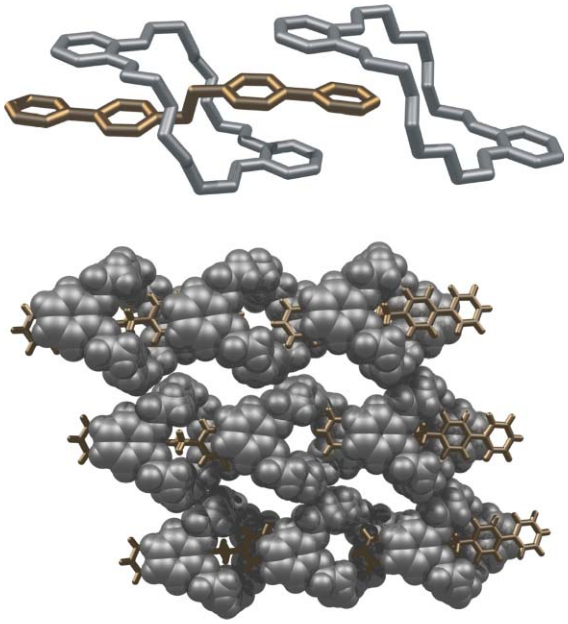

Fig. 17 The X-ray crystal structure of the 1D MORF with **RL1** units held together by hydrogen-bonding showing (top) the repeating unit and (bottom) three parallel strands.

In the case of the 3D MORFs, powder XRD patterns of the stable desolvated phase were consistent with retention of the 3D framework observed in the single crystal structures. Although the 1D and 2D materials do not retain their original lattices, the polyrotaxane frameworks remain intact as evidenced by the observation of a stable phase over a ~150 °C range prior to loss of crown ether. We can confidently conclude that these new materials are at least as stable as basic coordination polymers and there is nothing inherently unstable about a MORF structure.

For this chemistry to evolve, we must be able to prepare truly robust MORFs. This is an issue that can be addressed by utilising stronger metal–ligand interactions and metal clusters as nodes following the well documented evolution of conventional MOF materials. We have already shown that rotaxane ligands such as **RL2**, with a terpy chelator, will allow metal complexation under extreme synthetic conditions. This type of approach should therefore greatly expand the synthetic conditions under which MORF assembly can be conducted and allow the preparation of materials with increased stability.

5.2 Porosity and internal properties

The challenge of creating porous MOF materials for a variety of applications such as gas storage and catalysis is ongoing and some tremendous progress has been made.[40] The contribution that MORF materials can make to this area is that of fine-tuning the internal properties of porous materials. For a conventional MOF, the properties of the internal cavities or channels are dictated by the chemical structure of the organic linkers which define the great majority of the internal surface area. In a MORF, this internal surface is primarily related to the nature of the cyclic component and not the linking backbone. So when a robust and porous MORF can be created, the axle and metal nodes will dictate the shape of the framework but the cyclic wheel will define the internal surface chemistry. It will then be a facile supramolecular event to replace, for example, hydrophobic groups on the exterior of one wheel with hydrophilic groups of another and thereby change the internal property of the material in a predictable fashion without altering the basic framework structure of the MORF.

5.3 Dynamics and controllable motion in the solid state

One of the ultimate goals for this chemistry is to create solid state materials that contain arrays of ordered molecular machines based on mechanically interlocked species. We have already created the molecules and observed their properties as individual entities in solution and learned how to create basic MORF structures. The next step in the development of these materials will be to prepare robust, crystalline materials with mechanically switchable components.[41] The future involves learning how to make these materials and determine the driving forces (chemical, electrochemical, photochemical, *etc.*) that are compatible with the chemical make-up of the material.

Acknowledgements

I would like to thank all the members of my research group who contributed to the success of the projects described in this review;, in particular, James Wisner, Jorge Tiburcio, Sarah Vella, Greg Davidson, Dennis Hoffart, Dave Tramontozzi, Amy Hubbard-Root, Roopa Patel, Norma Georges and Neal Parekh. The Natural Sciences and Engineering Research Council of Canada, the Canadian Foundation for Innovation and the Petroleum Research Fund are thanked for financial support.

References

1 F. Arico, J. D. Badjic, S. J. Cantrill, A. H. Flood, K. C.-F. Leung, Y. Liu and J. F. Stoddart, *Top. Curr. Chem.*, 2005, **249**, 203 and references therein.
2 S. J. Loeb and J. A. Wisner, *Angew. Chem., Int. Ed.*, 1998, **37**, 2838.
3 B. L. Allwood, N. Spencer, H. Shahriari-Zavareh, J. F. Stoddart and D. J. Williams, *J. Chem. Soc., Chem. Commun.*, 1987, 1064.
4 S. J. Loeb, J. Tiburcio, S. J. Vella and J. A. Wisner, *Org. Biomol. Chem.*, 2006, **4**, 667.
5 G. J. E. Davidson, S. J. Loeb, N. A. Parekh and J. A. Wisner, *J. Chem. Soc., Dalton Trans.*, 2001, 3135 and references therein.
6 S. J. Loeb and J. A. Wisner, *Chem. Commun.*, 1998, 2757.
7 F. Huang and H. W. Gibson, *Prog. Polym. Sci.*, 2005, **30**, 982 and references therein.
8 J. W. Lee and K. Kim, *Top. Curr. Chem.*, 2003, **228**, 111 and references therein.
9 S. J. Loeb and J. A. Wisner, *Chem. Commun.*, 2000, 845.
10 S. J. Loeb and D. A. Tramontozzi, *Org. Biomol. Chem.*, 2005, **3**, 1393.
11 A. L. Hubbard, G. J. E. Davidson, R. H. Patel, J. A. Wisner and S. J. Loeb, *Chem. Commun.*, 2004, 138.
12 V. Balzani, A. Credi, F. M. Raymo and J. F. Stoddart, *Angew. Chem., Int. Ed.*, 2000, **39**, 3348.
13 S. J. Vella, J. Tiburcio, J. W. Gauld and S. J. Loeb, *Org. Lett.*, 2006, **8**, 3421.
14 S. J. Loeb and J. A. Wisner, *Chem. Commun.*, 2000, 1940.
15 A. M. Elizarov, S.-H. Chiu and J. F. Stoddart, *J. Org. Chem.*, 2002, **67**, 9175.
16 S. J. Loeb, J. Tiburcio and S. J. Vella, *Chem. Commun.*, 2006, 1598.
17 C. A. Hunter, *Angew. Chem., Int. Ed.*, 2004, **43**, 5310.
18 N. Georges, S. J. Loeb, J. Tiburcio and J. A. Wisner, *Org. Biomol. Chem.*, 2004, **2**, 2751.
19 K. Chichak, M. C. Walsh and N. R. Branda, *Chem. Commun.*, 2000, 847.
20 G. J. E. Davidson and S. J. Loeb, *Dalton Trans.*, 2003, 4319.
21 G. J. E. Davidson, S. J. Loeb, P. Passaniti, S. Silvi and A. Credi, *Chem.–Eur. J.*, 2006, **12**, 3233.
22 S. Bonnet, J.-P. Collin, M. Koizumi, P. Mobian and J.-P. Sauvage, *Adv. Mater.*, 2006, **18**, 1239 and references therein.
23 A. R. Pease, J. O. Jeppesen, J. F. Stoddart, Y. Luo, C. P. Collier and J. R. Heath, *Acc. Chem. Res.*, 2001, **34**, 433.
24 J.-P. Collin, C. Dietrich-Buchecker, P. Gaviña, M. C. Jiminez-Molero and J.-P. Sauvage, *Acc. Chem. Res.*, 2001, **34**, 477.
25 A. N. Shipway and I. Willner, *Acc. Chem. Res.*, 2001, **34**, 421.
26 R. Ballardini, V. Balzani, A. Credi, M. T. Gandolfi and M. Venturi, *Acc. Chem. Res.*, 2001, **34**, 445 and references therein.
27 H.-R. Tseng, D. Wu, N. X. Fang, X. Zhang and J. F. Stoddart, *ChemPhysChem*, 2004, **5**, 111 and references therein.
28 H. Yu, Y. Luo, K. Beverly, J. F. Stoddart, H.-R. Tseng and J. R. Heath, *Angew. Chem., Int. Ed.*, 2003, **42**, 5706.
29 H. W. Gibson, D. S. Nagvekar, M. Yamaguchi, S. Bhattacharjee, H. Wang, M. J. Vergne and D. M. Hercules, *Macromolecules*, 2004, **37**, 7514 and references therein.
30 O. M. Yaghi, M. O'Keefe, N. W. Ockwing, H. K. Chae, M. Eddaoudi and J. Kim, *Nature*, 2003, **423**, 705 and references therein.
31 The term MORF is used in this article to designate a sub-class of MOF as defined by Yaghi. See: J. L. C. Rowsell and O. M. Yaghi, *Microporous Mesoporous Mater.*, 2004, **73**, 3.
32 The preparation of these materials pre-dates those described herein. For an excellent review of this chemical system see: K. Kim, *Chem. Soc. Rev.*, 2002, **31**, 96.
33 G. J. E. Davidson and S. J. Loeb, *Angew. Chem., Int. Ed.*, 2003, **42**, 74.
34 J. Stahl, J. C. Bohling, E. B. Bauer, T. B. Peters, W. Mohr, J. M. Martín-Alvarez, F. Hampel and J. A. Gladysz, *Angew. Chem., Int. Ed.*, 2002, **41**, 1871 and references therein.
35 D. J. Hoffart, MSc thesis, University of Windsor, Windsor, Ontario, Canada, 2004.
36 D. J. Hoffart and S. J. Loeb, *Angew. Chem., Int. Ed.*, 2005, **117**, 901.
37 J.-R. Li, X.-H. Bu and R.-H. Zhang, *Inorg. Chem.*, 2004, **43**, 237 and references therein.
38 D. J. Hoffart and S. J. Loeb, *Supramol. Chem.*, 2007, **19**, DOI: 10.1080/10610270600979165.
39 J. Tiburcio, G. J. E. Davidson and S. J. Loeb, *Chem. Commun.*, 2002, 1282.
40 U. Mueller, M. Schubert, F. Teich, H. Puetter, K. Schierle-Arndt and J. Pastre, *J. Mater. Chem.*, 2006, **16**, 626.
41 For an review on creating molecular machines in the crystalline state see: T.-A. V. Khuong, J. E. Nuñez, C. E. Godinez and M. A. Garicia-Garibay, *Acc. Chem. Res.*, 2006, **39**, 413.